DOI: 10.1002/cbic.200700682

Small-Molecule Inhibitors of Sodium Iodide Symporter Function

Nathalie Lecat-Guillet,[a] Goulven Merer,[a] Roman Lopez,[a] Thierry Pourcher,[b] Bernard Rousseau,[a] and Yves Ambroise*[a]

The Na^+/I^- symporter (NIS) mediates iodide uptake into thyroid follicular cells. Although NIS has been cloned and thoroughly studied at the molecular level, the biochemical processes involved in post-translational regulation of NIS are still unknown. The purpose of this study was to identify and characterize inhibitors of NIS function. These small organic molecules represent a starting point in the identification of pharmacological tools for the characterization of NIS trafficking and activation mechanisms. The screening of a collection of 17020 druglike compounds revealed new chemical inhibitors with potencies down to 40 nM. Fluorescence measurement of membrane potential indicates that these inhibitors do not act by disrupting the sodium gradient. They allow immediate and total iodide discharge from preloaded cells in accord with a specific modification of NIS activity, probably through distinct mechanisms.

Introduction

The sodium/iodide symporter (NIS) is an intrinsic membrane glycoprotein that catalyzes the active accumulation of iodide from blood into the thyroid follicular cells. This transport represents the first step in the biosynthesis of thyroid hormones T4 and T3 which regulate many biological processes.[1] Other monovalent anions, such as ClO_4^-, SCN^-, and BF_4^- are also transported by the Na^+/I^- symporter.[2,3] The NIS is located in the basolateral membrane of thyrocytes and concentrates iodide against a 20- to 40-fold chemical gradient. The Na^+ gradient is the driving force for I^- transport and is maintained by the ouabain-sensitive Na^+/K^+ ATPase. NIS characterization at the molecular level has been made by cloning the rat, human, mouse, and porcine forms.[4–7] The human NIS is a 643-residue polypeptide, and was proposed to have 13 transmembrane segments.[8] Subcellular localization, expression, and activity of NIS was also shown to be regulated by thyroid-stimulating hormone (TSH)[9] through diverse control mechanisms including phosphorylation by regulatory proteins.[10] In a recent study, S43, T49, S227, T577, and S581 were identified as in vivo phosphorylation sites, and it was proposed that the phosphorylation status of these amino acid residues is correlated with the functional activity of NIS.[11] Taken together, these studies indicate that NIS maturation, localization, and activity are modulated at the post-translational level. Since the discovery of NIS, thorough biochemical analysis has elucidated the mechanism of basolateral iodide transport[12,13] and revealed the key role of NIS in thyroid diseases such as thyroid cancer, autoimmune disease, and congenital hypothyroidism.[14] Furthermore, the application of NIS as a novel cytoreductive gene strategy has opened up a promising field of research for the diagnosis and therapy of cancer outside the thyroid gland.[15]

Although many efforts have been made to characterize the sodium iodide symporter, little is known about the trafficking, activation, or deactivation mechanisms. Small organic inhibitors of iodide uptake can be used to generate bifunctional photoaffinity probes that may lead to the identification of NIS partners or other proteins that are involved in the regulation of iodide uptake.[16] NIS-directed molecules designed for affinity chromatography may lead to new approaches in protein purification and would allow testing of NIS function after reconstitution in a totally controlled environment. Such compounds may also be interesting for the diagnosis and treatment of thyroid dysfunction, or in the case of human contamination, by radioactive iodine species.[17]

Our approach to identify human NIS (hNIS) blockers involved high-throughput screening of a diverse compound collection. For this study, a fully automated radioiodide uptake assay was established for the rapid and quantitative screening of individual compounds in a 96-well format. We used a methodology based on the measurement of $^{125}I^-$ uptake in HEK293 cells permanently transfected with hNIS. The primary screen of a 17020-member library identified 61 hits. The compounds were subjected to extensive secondary analysis and chemical characterization. Ten new inhibitors were identified that block iodide uptake in the submicromolar to micromolar range by disrupting NIS function.

[a] *Dr. N. Lecat-Guillet, G. Merer, Dr. R. Lopez, Dr. B. Rousseau, Dr. Y. Ambroise*
Department of Bioorganic Chemistry and Isotopic Labelling, CEA
Institute of Biology and Technology (iBiTecS)
Gif-sur-Yvette 91191 (France)
Fax: (+33) 1-69-08-79-91
E-mail: yves.ambroise@cea.fr

[b] *Dr. T. Pourcher*
Department of Biochemistry and Nuclear Toxicology
University of Nice Sophia Antipolis
Nice 06107 (France)

Results

High-throughput screening of a 17020-compound library

The screen of the full library was performed by using an automated radioiodide uptake assay developed by our research group.[18] Radioiodide taken up by HEK293 cells expressing the human Na^+/I^- symporter can be easily determined by scintillation counting. In our previous work, the functional capacity of hNIS-HEK293 cells was demonstrated by isotopic flux measurements. The time course of iodide entrapment was shown to reach a steady state after 90 min at room temperature, indicating that efflux and influx of iodide occurred at the same rate. Quantitative evaluation of trapped versus total iodide at 120 min was calculated to be $>20\%$, representing a ~70-fold gradient of iodide. Perchlorate at 50 μM was shown to strongly decrease NIS-mediated iodide uptake and to trigger iodide discharge on preloaded cells by specific NIS inhibition. Furthermore, we demonstrated that iodide uptake was sodium dependent, ouabain sensitive, and strongly reduced at $+4\,^{\circ}C$. All these experiments demonstrated that iodide accumulation in HEK293 cells was quantitatively due to the presence of functional hNIS.[18] Additional evidence was obtained by measuring the inhibitory potencies of anions that block iodide translocation by competition for the iodide binding and transport site of NIS. The results revealed the following series: $PF_6^- > ClO_4^- > BF_4^- > SCN^- \gg NO_3^- > IO_4^- > N_3^- \gg Br^-$, in agreement with published results.[2,3]

In the primary screen, each compound was tested at a final concentration of 50 μM on confluent hNIS-HEK293 monolayer cell cultures. This yielded 163 compounds that inhibited iodide uptake by $>90\%$, representing a hit rate of 1%. The results of a representative set of 20 plates are shown in Figure 1. The

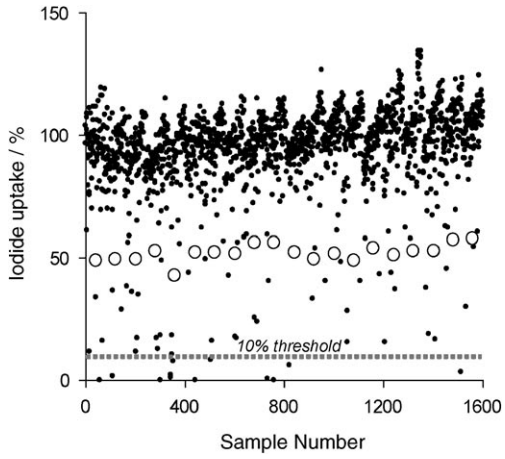

Figure 1. Primary high-throughput screen (HTS) results: data (●) from a representative set of 20 plates showing iodide uptake in hNIS-HEK293 cells after an incubation time of 2 h with $Na^{125}I$ (10 μM, 0.5 μCi per well) and the library compound (50 μM). Averaged iodide uptake ($n=4$) in the presence of ClO_4^- at 10^{-6} M is also shown (○). Data were normalized for each plate using the mean value of eight negative controls (no compound) and are shown as a percentage. Hits were defined as those that blocked iodide uptake by $>90\%$. In this initial series, 1600 samples were tested, and 12 hits were identified.

Z factor calculated over the entire HTS was 0.5, indicating a good degree of confidence in the biological activities assumed by both a high signal dynamic range and low data variation.[19] We then generated a new set of plates for re-screening the 163 hits along with a few weaker inhibitors having unique structural characteristics. Re-screening of the selected compounds was performed twice independently and at four different concentrations (5×10^{-5} M, 5×10^{-6} M, 5×10^{-7} M, and 5×10^{-8} M). We found that 61 compounds strongly and consistently inhibited iodide uptake at 50 μM in both confirmation screens. Preliminary IC_{50} values ranged from 2×10^{-5} M to 5×10^{-7} M. These 61 best compounds were selected for further characterization. Chlorofluoro(hydroxybenzyl)anilines, tetrahydro-β-carbolines, and dihydropyrimidinones were the most represented families, and other compounds having unique structural features were also identified.

False-positive elimination and purity/identity verification

A series of secondary assays was established to characterize false positives within the 61-member sub-library. A first test was set up for the identification of compounds that may quench the radioactive signal. Solid and liquid scintillation detection can suffer from quenching, a phenomenon that decreases the light output from the sample. In this context, scintillation quenching consists of either chemical quenching, in which other substances compete for the energy of the radiation, or color quenching, in which substances absorb the primary or secondary light emission.[20] To eliminate such compounds, we measured the radioactivity of a solution of $Na^{125}I$ (10 μM, 0.5 μCi per well) in a 96-well ScintiPlate with no cells in the presence of the tested compounds (50 μM), and compared the data with negative controls (that is, no compounds). We found that none of the 61 samples quenched the ^{125}I radioactive signal.

A second assay was set up for the titration of free iodide in the compound samples. Any overload of free iodide is unwanted in our assay, as it results in isotopic dilution of ^{125}I and signal decrease. Library suppliers generally report a sample purity of $>85\%$ from LC–MS and/or ^1H NMR analysis, two techniques that cannot measure inorganic species. Unfortunately, the presence of inorganic salts in compound samples is common, considering the technical difficulties of purifying the great number of molecules generated by combinatorial chemistry and parallel synthesis. In this context, the 61 samples were assayed for the presence of iodide by using the Sandell–Kolthoff reaction.[21] The method uses the very specific catalytic effect of iodide on the reduction of the yellow cerium ion (Ce^{4+}) to colorless Ce^{3+} by arsenious acid (As^{3+}). Six samples revealed significant amounts of iodide, corresponding to a 15–75 μM overload of "cold" iodide during the primary screen. These compounds were abandoned.

To narrow the number of compounds for further biochemical studies, we categorized compounds into classes of chemically related molecules by visual inspection. For each structural class we chose one or two compounds with the best efficiency (IC_{50} value), assuming that other compounds in the same class

act by the same mechanism of action. We also selected compounds on the basis of attractive chemical features, including chemical stability, water solubility, and ease of synthesis. The resulting sub-library of 14 compounds was re-supplied (Chembridge) and analyzed by ^{1}H NMR and LC–MS for purity and verification of identity. Ten samples were found to conform to the expected compound with $>95\%$ purity (Figure 2); these

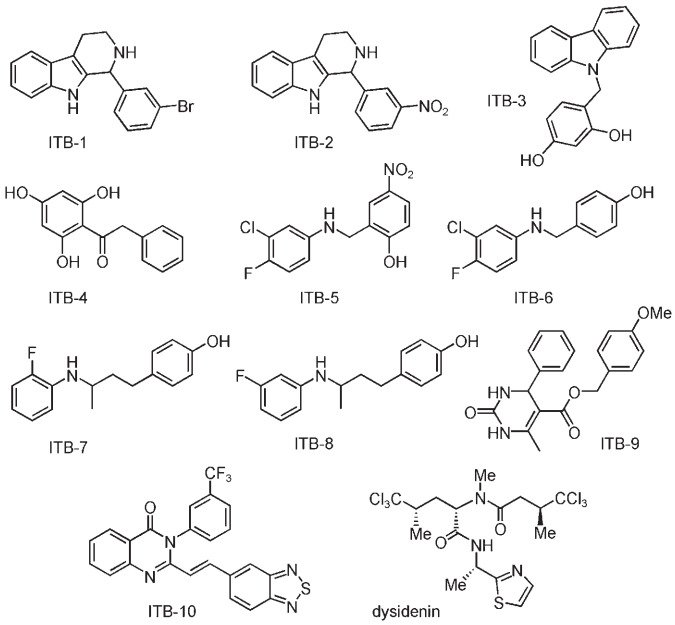

Figure 2. Structures of the most potent iodide uptake inhibitors; dysidenin is also shown.

were named ITB-1 to ITB-10 for "iodide transport blocker". The four other samples contained significant amounts of byproduct resulting from compound degradation or incomplete purification and were consequently abandoned.

Concentration-dependent inhibition of iodide uptake

For each of the 10 compounds (ITB-1 to ITB-10), we established the dose–response curve in hNIS-HEK293 cells as well as in the rat thyroid-derived cell line FRTL5 (Figure 3). Inhibition of iodide uptake in hNIS-HEK293 cells was dependent on compound concentration, with IC_{50} values from 0.4 μM (ITB-9) to 12 μM (ITB-6), confirming that the screen had identified potent inhibitors. Hill slopes were close to 1 ± 0.3. In comparison, the positive control ClO_4^- inhibited iodide uptake with an IC_{50} value of 1 μM. Concentration-dependent inhibition in FRTL5

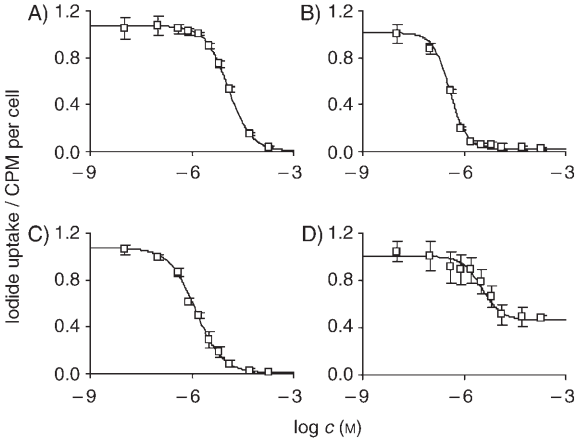

Figure 3. Dose-response curves of A) ITB-6, B) ITB-9, C) $NaClO_4$, and D) dysidenin on hNIS-HEK293. hNIS-HEK293 cells in 96-well plates (Isoplate-96) were incubated at 20 °C for 60 min (dysidenin was incubated for 120 min) with the indicated compounds (at 1.10^{-8}–1.10^{-4} M) in the presence of $Na^{125}I$ (10 μM, 0.2 μCi per well). Cells were washed at 4 °C before EtOH (30 μL) was added. Cell-associated radioactivity (expressed as counts per min (CPM) per cell) was determined after the addition of scintillation cocktail followed by gentle shaking overnight. Shown are the results of one experiment representative of at least three independent experiments with mean values ±SD ($n=4$). Experimental data were fitted by nonlinear regression to the four-parameter sigmoidal Hill equation using an "in-house" application developed in Visual Basic for Excel.

cells was also established for compounds ITB-1–ITB-10, and the activities were significantly better, with IC_{50} values ranging from 40 nM (ITB-5) to 1.3 μM (ITB-6) (Table 1). Dysidenin was also tested as a reference compound, and we observed that incubation for 120 min was necessary (no inhibition at 60 min) to obtain only partial inhibition (~50%) of iodide uptake in hNIS-HEK293 cells, whereas complete inhibition was observed for the FRTL5 cell line. Moreover, large variability in the data was always observed in assays of dysidenin ($n>4$), in contrast to the ITB compounds.

Fluorescence measurements of membrane potential

We measured the influence of ITB-1–ITB-10 on membrane potential of cultured hNIS-HEK293 cells using the voltage sensor probes CC2-DMPE and $DiSBAC_2(3)$. We found that neither our inhibitors (50 μM) nor ClO_4^- (50 μM) provoked significant variations on the fluorescence emission ratio 460 nm/580 nm, showing that there was no alteration of the membrane polarization status. Ouabain at 50 μM progressively depolarized the membranes within the first 35 min as a result of Na^+/K^+

Table 1. IC_{50} values of ITB-1–ITB-10, dysidenin, and $NaClO_4$ in hNIS-HEK293 and FRTL5 cells.

	IC_{50} [μM]											
Cell line	ITB-1	ITB-2	ITB-3	ITB-4	ITB-5	ITB-6	ITB-7	ITB-8	ITB-9	ITB-10	$NaClO_4$	dysidenin
hNIS-HEK293	2	3	0.7	9	3	12	6	4	0.4	7	1	2[a]
FRTL5	0.4	0.3	0.3	1	0.04	1.3	0.6	0.3	0.4	2	0.2	6

[a] Necessitated longer incubation time; partial inhibition.

ATPase inhibition and sodium redistribution across the plasma membrane.

Time-dependent inhibition of iodide uptake

We monitored time-dependent iodide uptake in hNIS-HEK293 cells in the presence of ITB-1–ITB-10, ClO_4^-, dysidenin, and ouabain. As expected, iodide uptake was immediately and totally blocked by ClO_4^- (50 μM) throughout the experiment (Figure 4). In contrast, 50 μM ouabain did not perturb NIS activity during the first 20 min before iodide was quantitatively discharged. We observed that ITB-1, ITB-2, ITB-10, and dysidenin showed a time-dependent iodide uptake profile similar to that of ouabain. In contrast, compounds ITB-3–ITB-9 inhibited iodide accumulation immediately and continuously, as if they directly blocked NIS-mediated iodide translocation.

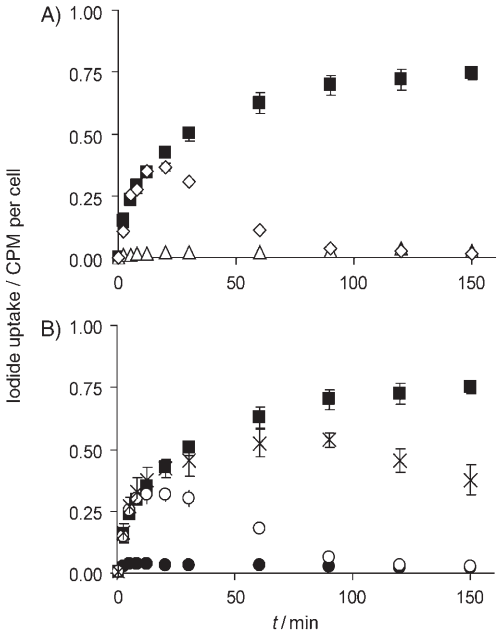

Figure 4. Time-dependent iodide uptake in hNIS-HEK293 cells in the presence of inhibitors. Iodide uptake was measured at 2, 5, 8, 12, 20, 30, 60, 90, 120, and 150 min on hNIS-HEK293 cells after incubation at 20 °C in the presence of $Na^{125}I$ alone (10 μM, 0.2 μCi per well, ■), and ITB-5 (●), ITB-10 (○), $NaClO_4$ (△), ouabain (◇), and dysidenin (×). For clarity, results are split (A and B). All inhibitors were tested at 50 μM. Shown are the results of a representative experiment with mean values ± SD ($n = 3$).

Compound-mediated iodide discharge and cell viability

We tested compounds ITB-1–ITB-10 for their ability to discharge iodide from preloaded hNIS-HEK293 cells (Figure 5). Rapid iodide efflux was observed in each case immediately after the addition of the inhibitor at 50 μM (only ITB-9 is shown). Iodide discharge was near complete (> 80%) after 60 min, and $NaClO_4$ (50 μM) was not significantly more potent than ITB compounds. In contrast, dysidenin mediated iodide efflux only after 60 min, and to a significantly lower extent (< 30%).

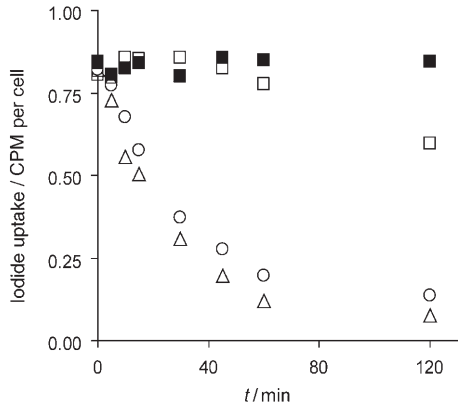

Figure 5. Time-dependent iodide efflux by ITB compounds. hNIS-HEK293 cells were incubated at 20 °C with $Na^{125}I$ (10 μM, 0.2 μCi per well) for 60 min before ITB-9 (○), $NaClO_4$ (△), dysidenin (□), and no compound (■) were added. All inhibitors were tested at 50 μM. Trapped iodide was measured at 5, 10, 15, 30, 45, 60, and 120 min after the addition of inhibitors, followed by overnight shaking in scintillation cocktail. The experiments are representative of two independent experiments. Standard deviation bars (< 5%, $n = 4$) are omitted for clarity.

hNIS-HEK293 cell viability was also tested in the presence of ITB-1–ITB-10. None of the selected compounds was toxic at concentrations up to 200 μM. In contrast, ouabain was toxic to the cells below 1 μM. The microplates were further allowed to stand for two additional days in the presence of compounds, and in each case cell growth was not affected.

Discussion

A small number of organic molecules have been reported to block iodide uptake in NIS-expressing systems. However, most of them are not specific for the Na^+/I^- symporter. Ouabain and other cardiotonic glycosides strongly decrease iodide uptake in thyroid cells through Na^+/K^+ ATPase inhibition.[22] These compounds abolish the energy required for iodide translocation by disrupting the Na^+ gradient across the lipid bilayer. Harmaline has been reported to inhibit iodide transport by competing for the sodium binding site of NIS.[23] However, harmaline is not selective and targets other Na^+-dependent transporters by the same mechanism.[24–26] Van Sande et al. reported in 1990 that dysidenin, a hexachlorinated peptide-derived molecule extracted from the toxic sponge *Dysidea herbacea*, can block iodide accumulation in dog thyroid slices,[27] in plasma membrane vesicles prepared from bovine thyroid,[28] and in rat thyroid cells.[29] From isotopic flux measurements, it was proposed that dysidenin is a "pseudocompetitive" inhibitor of NIS. However, the structural complexity of the marine toxin has discouraged chemists from proposing a synthetic methodology amenable to chemical modifications. For this reason, dysidenin has never been used as a chemical tool to characterize or isolate the NIS molecule.

We have used an automated high-throughput screen of a 17020-compound library to identify a series of potent inhibi-

tors of NIS-mediated iodide transport. The selection was based on the magnitude of iodide uptake inhibition in HEK293 cells expressing the human sodium/iodide symporter (hNIS-HEK293). The screening was successful in 100% of the 96-well plates as determined by $^{125}I^-$ transport measurements in positive (with ClO_4^-) and negative (no compound) controls. A total of 61 chemical samples were selected after re-screening the hits at different concentrations. The presence of iodide was examined in the 61 samples by the Sandell–Kolthoff method. The results showed that six samples were contaminated with free iodide in quantities sufficient to cause isotopic dilution during the assay, and these were therefore discarded. An additional round of selection was performed. Several members were eliminated on the basis of structural similarities, leaving one or two compounds representing each chemical class. Finally, 14 compounds were re-supplied in milligram quantities for secondary analysis. Because the quality and stability of each member of a large chemical library is difficult to check, it was essential to verify compound identities and purities. ^{1}H NMR and LC–MS analysis identified ten samples with satisfactory purities (>95%), and eliminated four samples containing undesirable by-products.

The ten inhibitors were evaluated on cultured rat thyroid-derived cell line FRTL5 and HEK293 expressing hNIS. The inhibition potencies were confirmed for all tested compounds in both cell lines, and IC_{50} values were found to be in the micromolar to sub-micromolar range (IC_{50} = 40 nM for ITB-5 on FRTL5). The superior inhibition potencies consistently observed in the rat thyroid cell line may be explained by discrepancies in the post-translational regulation of the transporter caused by lower expression of regulator proteins and/or higher NIS protein levels in HEK293 relative to FRTL5 cells. None of the inhibitors showed cellular toxicity in its respective range of activity. Seven compounds were found to have an immediate effect on iodide uptake (ITB-3 to ITB-9). By comparison with the time-dependent inhibition profile of iodide uptake by the Na^+/K^+ pump inhibitor ouabain, it is unlikely that they disrupt the sodium gradient. Three other compounds (ITB-1, ITB-2, and ITB-10) were found to provoke a delayed inhibition similar to that of ouabain, a result that may suggest a sodium gradient disruption mechanism. However, these three compounds are not toxic toward cells at concentrations up to 200 μM, whereas ouabain provokes cell death at sub-micromolar concentrations (not shown). These results suggest that ITB-1, ITB-2, and ITB-10 do not disrupt the membrane sodium gradient, which is essential for cell viability. To verify this hypothesis, we tested compounds ITB-1–ITB-10 for their influence on membrane potential using the voltage sensor probes CC2-DMPE and $DiSBAC_2(3)$.[30] None of the inhibitors was found to depolarize the plasma membrane on hNIS-HEK293. This result shows that the sodium gradient is maintained during iodide uptake disruption, and strongly suggests that ITBs are direct inhibitors of NIS activity.

The 10 inhibitors immediately discharged iodide preloaded cells, and no lag phase was observed. This result suggests the presence of dynamic mechanisms that maintain NIS activity. Nevertheless, a direct and disruptive binding of the inhibitor on the symporter cannot be excluded. The differences in the inhibition behavior observed in the time-dependent inhibition experiments (Figure 4, Table 2) between ITB-1, ITB-2, and ITB-10 on one hand, and ITB-3–ITB-9 on the other, may be explained by the presence of distinct mechanisms for the disruption of NIS activity.

Table 2. Inhibition characteristics of the inhibitors.[a]

Immediate inhibition	Delayed inhibition
3, **4**, **5**, **6**, **7**, **8**, **9**, $NaClO_4$	**1**, **2**, **10**, dysidenin, ouabain

[a] The inhibitors are categorized according to their action toward NIS-mediated iodide uptake.

Previous studies have suggested that the marine toxin dysidenin is an inhibitor of the Na^+/I^- symporter. Herein, we found that the inhibition of iodide uptake by dysidenin was incomplete (~50%) in HEK293 cells expressing hNIS, whereas it was complete in FRTL5. We also noticed that the marine toxin required prolonged incubation times for observable inhibition. This behavior was confirmed in measurements of time-dependent I^- accumulation in the presence of dysidenin: no inhibition was detected during the first 30 min before weak inhibition occurred. Dysidenin also mediated a poor and deferred iodide discharge of preloaded hNIS-HEK293 cells. These results are not compatible with a specific inhibition of the Na^+/I^- symporter, although we cannot exclude the presence of a selective action of the marine toxin for the murine, canine, and bovine forms over the human form of NIS. Nevertheless, the poor aqueous solubility of dysidenin (cloudy solution at 20 μM) should be considered in the interpretation of biological activity. The in silico prediction of its partition coefficient ($\log P > 5$)[31] provides strong evidence for considerable solubilization in membranes, a potential cause of the perturbation of ion permeation.

Conclusions

The small-molecule inhibitors identified herein will allow a broad investigation of the intracellular signaling pathways in which they are involved. Their simple structure is amenable to the preparation of radioactive or biotinylated photoprobes designed for the identification and purification of target proteins. They also represent lead compounds for the synthesis of new anti-thyroid drugs. Chemical modifications are possible, and the preparation of derivatives with improved drug properties such as higher activity, greater specificity, and improved ADMET characteristics offers considerable opportunities for the treatment of thyroid dysfunction.

Experimental Section

Chemicals and solutions: Carrier-free $Na^{125}I$ (GE Healthcare, Chalfont St. Gilles, UK) was diluted with distilled water (5 mCi mL^{-1}). This stock solution was kept at room temperature and used for no

more than two months. The uptake buffer consisted of a Hank's balanced salt solution (HBSS, Sigma–Aldrich) supplemented with HEPES (10 mM, Sigma–Aldrich). Stock solutions of positive control ClO_4^- (Sigma) were prepared by dilution in the uptake buffer (HBSS/HEPES 10 mM) at 10× the final concentration and stored at +4 °C for up to one week. Working solutions of NaI/$Na^{125}I$ (100 μM, 50 μCi mL^{-1}) in uptake buffer (HBSS/HEPES 10 mM) were prepared daily. A sample consisting of a mixture of isodysidenin/dysidenin (7:3) extracted from *Dysidea herbacea* was kindly provided from Prof. J.-C. Braekman (Université libre de Bruxelles, Belgium) and was subsequently purified by HPLC. Briefly, a sample (50 mg) was passed through a Zorbax-SIL column (25 cm×21.4 mm) eluting with $CHCl_3$/hexanes/MeOH 60:40:0.1 at 5 mL min^{-1}. Pure dysidenin (13 mg) was collected between 26.4 and 44.0 min, and characterized by LC–MS, ^{13}C NMR, ^1H NMR, and polarimetry.[32]

Cell lines: HEK293 cells stably expressing the human Na^+/I^- symporter (hNIS) were cultured in Dulbecco's modified Eagle's medium (DMEM, Invitrogen) supplemented with 10% heat-inactivated fetal bovine serum (Invitrogen), 2 mM L-glutamine (Sigma), 100 U mL^{-1} penicillin (Sigma), 0.1 mg mL^{-1} streptomycin (Sigma) at 37 °C, and 5% CO_2. FRTL5 cells (generously provided by Prof. B. Rousset, INSERM, Lyon, France) were cultured as described elsewhere with slight modifications.[33] Briefly, FRTL5 cells were cultured in Coon's modified F12 medium (Biochrom) supplemented with 5% heat-inactivated fetal bovine serum (Invitrogen), 2 mM L-glutamine (Sigma), 100 U mL^{-1} penicillin (Sigma), 0.1 mg mL^{-1} streptomycin (Sigma), 10 μg mL^{-1} insulin (Sigma), 10 nM hydrocortisone (Sigma), 10 ng mL^{-1} Gly-His-Lys acetate (Sigma), 1 mU mL^{-1} TSH (Sigma), 5 μg mL^{-1} transferrin (Sigma) at 37 °C, and 5% CO_2. For iodide uptake assays, hNIS-HEK293 cells (3.5×10^4 cells per well) and FRTL5 cells (4×10^4 cells per well) were plated in 96-well microtiter plates (Isoplate-96 or ScintiPlate-96, PerkinElmer) using a Multidrop 384 instrument (Thermo Labsystems) and cultured for three days to reach a confluent monolayer cell culture. For the HEK293 cell line, microtiter plates were previously treated with poly-L-lysine (Sigma) to prevent cell wash-out.

High-throughput screening: The chemical library (Diverset, Chembridge) consisted of a diverse collection of 17020 druglike small molecules representing a biologically relevant pharmacophore diversity space. The compounds were provided in 96-well plates at 10 mM in DMSO. For screening, bar-coded daughter plates were prepared at 500 μM by dilution with uptake buffer (HBSS/HEPES 10 mM). Each daughter plate contained 80 different individual compounds, with the first and last columns used for negative (5% DMSO in uptake buffer) and positive ($NaClO_4$: 10^{-6} M, 10^{-5} M, 10^{-4} M) controls. Final DMSO content was 0.5%. We observed that DMSO had no significant effect on iodide uptake up to a concentration of 2%. Screening was carried out on a Genesis workstation 200 (Tecan) equipped with a Carousel BC (Tecan), a Cytomat 2C cell incubator (Kendro), a microtiter plate washer PW384 (Tecan), and a 6-detector Microbeta Trilux microplate β-counter (Perkin Elmer). The system was controlled using Gemini 4.00 and FACTS 4.81 software packages (Tecan). Output files were generated from FACTS software in text (.txt) format. Data were analyzed using a custom application developed using Microsoft Visual Basic for Excel.

Optimization and validation procedures of the automated assay are described in detail elsewhere.[18] The high-throughput screen was performed on hNIS-HEK293 cells plated on poly-L-lysine-coated 96-well ScintiPlates (PerkinElmer). Briefly, daughter plates with compounds and controls as well as working microplates (with cells) were loaded in the carousel, and the automated sequence was initiated. Confluent cell culture microplates were washed (PW384) with uptake buffer (HBSS/HEPES 10 mM) such that 80 μL per well of fresh buffer remained at the end of the cycle. Compounds and controls from daughter plates were distributed (10 μL per well), followed by 10 μL per well of the NaI/$Na^{125}I$ working solution (100 μM, 50 μCi mL^{-1}). The microplates were left to stand at 20±1 °C for 2 h, then washed (PW384) with the uptake buffer (HBSS/HEPES 10 mM) and each well was counted for radioactivity (Microbeta Trilux).

Compound toxicity: hNIS-HEK293 cells were plated in 96-well clear polystyrene microplates (3.5×10^4 cells per well) using the Multidrop 384 and allowed to grow for 2 days at 37 °C and 5% CO_2. The compounds as well as ouabain (final concentrations of 1, 5, 50, and 200 μM) were added such that the final volume was 200 μL, and the cell culture was allowed to stand for one additional day at 37 °C and 5% CO_2. The effect of compounds on cell growth was quantified by the resazurin test and compared with reference wells with no compounds.[34] Briefly, 40 μL of a resazurin (Sigma) solution (0.48 mM in PBS) was added to each well, and the plates were allowed to stand for 5 h at 37 °C and 5% CO_2. Fluorescence signals ($\lambda_{ex}=560$ nm) at 590 nm were recorded on a Spectramax Gemini XS microplate spectrofluorometer (Molecular Devices), and compared with those of wells with no compounds (0.5% DMSO).

Iodide detection in compound samples and scintillation quenching: Iodide concentration was determined using the modified Sandell–Kolthoff method.[21] Samples were tested in 96-well clear polystyrene microplates by diluting stock solutions of compounds in NaCl (4 g L^{-1}), sodium arsenite (8 mM, prepared from As_2O_3 and NaOH) in a total volume of 230 μL per well. The reaction was started after the addition (20 μL per well) of a solution consisting of ammonium cerium(IV) sulfate (40 mM) in sulfuric acid (3.6 N). The absorbance at 420 nm was recorded on a SpectraMax Plus 384 instrument (Molecular Devices) after 20 min and compared with KI standards (0, 5, 10, 15, 20, 25, 30 μg L^{-1}). The absence of scintillation quenching due to the compound was checked in 96-well ScintiPlates. The compounds (50 μM final) and $Na^{125}I$ (10 μM, 0.5 μCi per well final) were distributed in the 96-well microplate such that the total volume did not exceed 30 μL, to ensure proximity with the solid scintillator incorporated into the bottom of the polystyrene plastic well. The radioactivity was measured (Microbeta Trilux) and compared with that of negative controls (no compound).

IC_{50} determination, time-dependent iodide influx and efflux: The concentration-dependent inhibition of iodide uptake was measured using a procedure similar to automated high-throughput screening with minor modifications. hNIS-HEK293 cells (3.5×10^4 cells per well) or FRTL5 cells (4×10^4 cells per well) were plated in Isoplate-96 (PerkinElmer) and allowed to grow at 37 °C and 5% CO_2 for three days. The selected compounds at various concentrations and $Na^{125}I$ (10 μM, 0.2 μCi per well final) were added successively to the monolayer cell culture in uptake buffer (HBSS/HEPES 10 mM). The plates were left to stand at 20±1 °C for 60 min (hNIS-HEK293) or 45 min (FRTL5) before the cells were washed with cold buffer (HBSS/HEPES 10 mM at +4 °C), and the remaining supernatant was discarded. EtOH (30 μL per well) and scintillation cocktail (160 μL per well, Analytic Unisafe 1, Zinsser) were successively added, and the plates were shaken overnight at room temperature before the radioactivity was measured (Microbeta Trilux). Time-dependent iodide uptake and discharge were measured on hNIS-HEK293 cells using the same procedure by varying the incubation time after the addition of compound (50 μM final) and $Na^{125}I$ (10 μM, 0.2 μCi per well final).

Fluorescence measurements of membrane potential: hNIS-HEK293 cells plated (3.5×10^4 cells per well) in poly-L-lysine-coated 96-well black-walled microplates were allowed to grow three days at 37 °C and 5% CO_2, and equilibrated in HBSS/HEPES (10 mM, 100 μL) as described above. The voltage sensor probes CC2-DMPE and $DiSBAC_2(3)$ were used according to manufacturer's instructions (Invitrogen). CC2-DMPE and $DiSBAC_2(3)$ were both at final concentrations of 4 μM for optimal readout. Background-corrected fluorescence signals ($\lambda_{ex}=410$ nm) at 460 nm and 580 nm were recorded immediately after the addition of compound for one hour using a Spectramax Gemini XS microplate spectrofluorometer (Molecular Devices).

Compound verification: LC–MS analysis was performed on a system equipped with a binary gradient solvent delivery system (2525, Waters), a sample injector (2767, Waters), a photodiode array detector (2996, Waters), an evaporative light-scattering detector (PL-ELS 1000, Polymer Laboratory), and an electrospray ionization mass spectrometer (Micromass-ZQ, Waters). Each selected compound (20 μg) was applied to a 10×4.6 mm X-terra 5 μm C_{18} (Waters) equilibrated with $CH_3CN/H_2O=5:95$ and 0.1% formic acid. Samples were eluted by increasing CH_3CN to 100% (8–13 min). ^1H NMR spectra were recorded on a Bruker Avance DPX 400 spectrometer in $[D_6]$DMSO.

Glossary: FRTL: Fischer rat thyroid low serum; HEK: human embryonic kidney; ADMET: absorption, distribution, metabolism, elimination, toxicity.

Acknowledgements

We are grateful to B. Rousset (INSERM, Lyon, France) for FRTL5 cell lines and J.-C. Braekman (University of Brussels, Belgium) for the generous gift of the dysidenin/isodysidenin extract mixture. We thank Dr. François Leuteutre (CEA-iBiTecS, Saclay, France) for critical reading of the manuscript and David Buisson (CEA-iBiTecS, Saclay, France) for performing the LC–MS analysis. This work was supported by CEA-iBiTecS.

Keywords: biological activity · high-throughput screening · inhibitors · membrane proteins · sodium iodide symporter

[1] S. P. Porterfield, C. E. Heindrich, *Endocr. Rev.* **1993**, *14*, 94–106.
[2] J. Wolff, *Physiol. Rev.* **1964**, *44*, 45–90.
[3] P. A. Jones, R. U. Pendlington, L. K. Earl, R. K. Sharma, M. D. Barrat, *Toxicol. in vitro* **1996**, *10*, 149–160.
[4] G. Dai, O. Levy, N. Carrasco, *Nature* **1996**, *379*, 458–460.
[5] P. A. Smanik, Q. Liu, T. L. Furminger, K. Ryu, S. Xing, E. L. Mazaferi, S. M. Jhiang, *Biochem. Biophys. Res. Commun.* **1996**, *226*, 339–345.
[6] B. Perron, A. M. Rodriguez, G. Leblanc, T. Pourcher, *J. Endocrinol.* **2001**, *170*, 185–196.
[7] S. Selmi-Ruby, C. Watrin, S. Trouttet-Masson, F. Bernier-Valentin, V. Flachon, Y. Munari-Silem, B. Rousset, *Endocrinology* **2003**, *144*, 1074–1085.
[8] O. Levy, A. De La Vieja, C. S. Ginter, C. Riedel, G. Dai, N. Carrasco, *J. Biol. Chem.* **1998**, *273*, 22657–22663.
[9] A. Paire, F. Bernier-Valentin, S. Selmi-Ruby, B. Rousset, *J. Biol. Chem.* **1997**, *272*, 18245–18249.
[10] C. Riedel, O. Levy, N. Carrasco, *J. Biol. Chem.* **2001**, *276*, 21458–21463.
[11] D. D. Vadysirisack, E. S. W. Chen, Z. Zhang, M. D. Tsai, G. D. Chang, S. M. Jhiang, *J. Biol. Chem.* **2007**, *282*, 36820–36828.
[12] O. Dohan, A. De La Vieja, V. Paroder, C. Riedel, M. Artani, M. Reed, C. S. Ginter, N. Carrasco, *Endocr. Rev.* **2003**, *24*, 48–77.
[13] G. Dai, O. Levy, L. M. Amzel, N. Carrasco in *Handbook of Biological Physics, Vol. 2: Transport Processes in Eukaryotic and Prokaryotic Organisms* (Eds.: W. N. Konings, H. R. Kaback, J. S. Lolkema), Elsevier, Amsterdam, **1996**, pp. 343–368.
[14] C. Schmutzler, J. Kohrle, *Exp. Clin. Endocrinol. Diabetes* **1998**, *106*, S1–10.
[15] G. Riesco-Eizaguirre, P. Santisteban, *Eur. J. Endocrinol.* **2006**, *155*, 495–512.
[16] Y. Hatanaka, Y. Sadakane, *Curr. Top. Med. Chem.* **2002**, *2*, 271–288.
[17] M. Dayem, V. Navarro, R. Marsault, J. Darcourt, S. Lindenthal, T. Pourcher, *Biochimie* **2006**, *88*, 1793–1806.
[18] N. Lecat-Guillet, G. Merer, R. Lopez, T. Pourcher, B. Rousseau, Y. Ambroise, *Assay Drug Dev. Technol.* **2007**, *5*, 535–540.
[19] J. H. Zhang, T. D. Y. Chung, K. R. Oldenburg, *J. Biomol. Screening* **1999**, *4*, 67–73.
[20] G. Simmonet, M. Oria in *Les Mesures de Radioactivité à l'Aide des Compteurs à Scintillateur Liquide* (Ed.: G. Simmonet), Eyrolles, Paris, **1990**, pp. 97–151.
[21] E. B. Sandell, I. M. Kolthoff, *J. Am. Chem. Soc.* **1934**, *56*, 1426–1426.
[22] J. Wolff, *Biochim. Biophys. Acta* **1960**, *38*, 316–324.
[23] S. M. Kaminsky, O. Levy, M. T. Garry, N. Carrasco, *Eur. J. Biochem.* **1991**, *200*, 203–207.
[24] M. S. Suleiman, R. C. Hider, *Mol. Cell. Biochem.* **1985**, *67*, 145–150.
[25] P. S. Aronson, S. E. Bounds, *Am. J. Physiol.* **1980**, *238*, F210–217.
[26] A. Mahmood, F. Alvarado, *Biochim. Biophys. Acta Enzymol.* **1977**, *483*, 367–374.
[27] J. Van Sande, F. Deneubourg, R. Beauwens, J.-C. Braekman, D. Daloze, J. E. Dumont, *Mol. Pharmacol.* **1990**, *37*, 583–589.
[28] L. Vroye, R. Beauwens, J. Van Sande, D. Daloze, J.-C. Braekman, P. E. Golstein, *Pfluegers Arch.* **1998**, *435*, 259–266.
[29] J. Van Sande, C. Massart, R. Beauwens, A. Schoutens, S. Costagliola, J. E. Dumont, J. Wolff, *Endocrinology* **2003**, *144*, 247–252.
[30] C. Wolff, B. Fuks, P. Chatelain, *J. Biomol. Screening* **2003**, *8*, 533–543.
[31] Calculated at http://www.vcclab.org/lab/alogps/ (accessed February 4, 2008).
[32] R. Kazlauskas, R. O. Lidgard, R. J. Wells, W. Vetter, *Tetrahedron Lett.* **1977**, *18*, 3183–3186.
[33] F. S. Ambesi-Impiombato, L. A. M. Parks, H. G. Coon, *Proc. Natl. Acad. Sci. USA* **1980**, *77*, 3455–3459.
[34] J. O'Brien, I. Wilson, T. Orton, F. Pognan, *Eur. J. Biochem.* **2000**, *267*, 5421–5426.

Received: November 10, 2007
Published online on February 28, 2008

